Electrochemical Study Of Nanostructured Trimanganese Tetroxide Synthesized Through A Single Step Auto Igniting Combustion Technique

Sherin J.S. [1]

[1]Department of Physics, All Saint's College, Trivandrum, Kerala, India.

Correspondence: Sherin J. S.

All Saint's College, Trivandrum, Kerala, India.

Abstract

Stable low cost environmentally benign Mn_3O_4 nanomaterial for supercapacitor application were synthesized by combustion method by concentration of the precursors. The formation of Mn_3O_4 nanoparticles were confirmed by x-ray diffraction (XRD), scaninnng electron microscopy (SEM) and energy dispersive absorption spectroscopy (EDAX) studies. The average particle size have been found to be about 40-45 nm. UV Visible spectroscopy results showed maximum transmittance in the visible regions, it revealed poor transmittance in the ultraviolet region. The electrochemical performance of Mn_3O_4 electrode was examined in poly-tetrafluoroethylene, which exhibited a high specific capacitance of 211 F/g at a scan rate of 1mV/s over a potential range -0.1V to 0.8V and showed excellent electrochemical stability during cycling. The capacitive retention of Mn_3O_4 electrode showed about 86% of the initial capacitance.The good conductivity and good cyclic stability suggested that Mn_3O_4 could be used as an electrode material in electrochemical capacitors.

Keywords: Nanocrystals, Supercapacitor, Cyclic voltammetry, Galvanostatic charge discharge cycle, EDAX, Trimanganese tetroxide.

1. Introduction

As a new energy storage device, supercapacitors (ECs) have awakened prodigious consideration due to its superior power delivery and cycling life compared to those of rechargeable batteries, and superior density delivery compared to those of conventional electrolytic capacitors [1]. Hence, ECs offer a promising method to meet the increasing power demands of energy storage systems [2-4].Based on the electrochemical behavior and charge/energy storage mechanisms, the supercapacitors are classified into, electrical double layer capacitors and pseudo-capacitors. Typical electrode materials that consist of metal oxides or conducting polymers, transfer faradic

charges between an electrolyte and electrode [5-7]. Composite materials based on metal oxides/conducting polymers have attracted a great deal of attention for their higher energy/power capability [8,10].

Among the various metal oxides, manganese oxide as a supercapacitor electrode has been extensively studied due to its high theoretical capacitance (1370Fg-1), low cost, low toxicity and resource abundance [9,11]. Manganese dioxide offers high pseudo capacitance through fast and reversible redox reactions near the surface of active materials [12]. The natural abundance and low cost of Mn oxides, along with their satisfactory energy-storage performance in mild electrolytes and environmental compatibility, has made them the most promising novel electroactive material for the pseudo capacitor applications. Mn_3O_4 can be synthesized via thermal decomposition, sol-gel processes, electrochemical deposition, solution-based chemical routes, and solid-state reactions.[13-16]. Changes in the synthesis parameters such as current density, temperature, reactant concentration and pH, results in different physical, chemical, and electrochemical properties of manganese oxide. The synthesis conditions determine the properties of the manganese oxide produced. Previously reported manganese oxides demonstrated specific capacitances as high as 600 Fg^{-1} for thin films and 150-300 Fg^{-1} for powder-based electrodes within a potential window of 0.9-1.2V in aqueous electrolytes containing KCl, K_2SO_4, NaCl, or Na_2SO_4[17-20]. Herein the present work, Mn_3O_4 nanopowder is synthesized using a single step auto igniting combustion technique, and consequently its structural, morphological, optical and electrochemical properties are investigated.

2. Experimental

In order to synthesize the Mn3O4 nanoparticles, stock solutions of Mn $(ClO_4)_2$. xH_2O (0.1 M) was dissolved in double distilled water as the starting reagent. Citric acid was then added to the solutions taken in separate beakers as a complexing agent. Amount of citric acid was calculated based on total valence of the oxidising and reducing agents for maximum release of energy during combustion. Oxidant to fuel ratio was adjusted to unity (~1) by adding concentrated nitric acid, which serves as an oxidiser, and ammonium hydroxide solution as fuel. The precursor solution of pH ~ 7.0 was stirred well for uniform mixing without any sedimentation. The solution was then heated using a hot plate kept at ~250^oC in a ventilated fume hood and the boiling solution underwent dehydration accompanied by foam. On persistent heating, the foam got auto ignited, producing voluminous fluffy grayish brown Mn_3O_4 nanopowder[21-24]. The synthesized samples were characterized for their structure by x-ray diffraction (PHILIPS XPERT-PRO) with Cu Kα radiation. Thermo Nicolet Model:6700 was used for FT-IR

spectral analysis. Scanning electron microscopy (JEOL Model JSM-6390LV) was utilized for analyzing the combustion product's particulate properties. The UV-Vis spectra of the samples were recorded using JASCO V 570 spectrophotometer in the wavelength range of 200 -900 nm. Electrochemical measurements were performed with an Autolab PGSTAT302N. The electrochemical cell was configured with a bright Platinum (Pt) electrode as the counter electrode and the reference electrode used was the Ag/Ag Cl electrode. A polished glassy carbon working electrode (GCE) of 5mm in diameter was used as the current collector. The working electrode for Mn_3O_4 was prepared by forming a slurry comprising of a mixture of Mn_3O_4 with polytetrafluoroethylene(PTFE) with a ratio of 85:10:5. A small amount of ethanol was added to make the mixture homogeneous. The slurry thus obtained was dried at 80^oC for 6 hours and pressed in Nickel foam as the current collector with 1M Na_2SO_4 solution employed as the electrolyte. Cyclic voltammetry (CV) and Galvanostatic charge –discharge measurements were performed over a potential range from -0.1V to 0.8V at various scan rates (5 to 50mV/S) and different current densities. All electrochemical experiments were conducted at room temperature.

3. Results and Discussion

3.1. *X-Ray diffraction Studies*

The XRD pattern of the as prepared Mn_3O_4 nanopowder at different pH through the combustion method is shown in figure 1.1. From the XRD pattern, it is clear that Mn_3O_4 exhibits tetragonal structure. All the peaks including the minor ones are indexed based on the JCPDS file 24-0734 for Mn_3O_4 nanoparticle. The strong and sharp peaks indicate that the as prepared nanopowders are highly crystalline. No secondary phase or impurity peak from other Mn-O phases or other by products originating from the synthesis procedure were detected in the XRD pattern which confirms that the as prepared powder itself is phase pure without any further processing. Thus, the present preparation technique offers an easy, time saving and economic approach for the synthesis of nanoparticles in a single step.

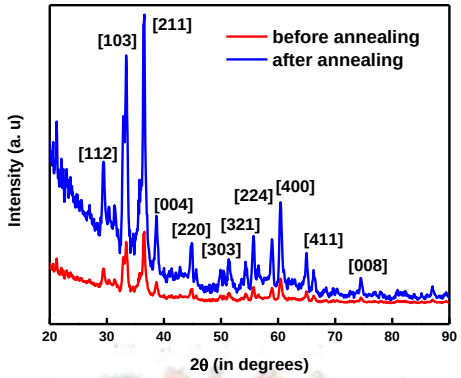

Fig 1.1 XRD pattern of Mn_3O_4 nanoparticle.

3.2 Morphological Studies

The surface morphology and particle size of the samples were examined using SEM image given in the figure 1.2 with two different magnifications micrographs of Mn_3O_4. The nanoparticles are agglomerated together to form a spherical shape with porous morphology within 40-45 nm range. In his work, Dubel et alpointed out that the spherical shaped nanocrystals have high surface morphology that can be useful for supercapacitor application.[4].

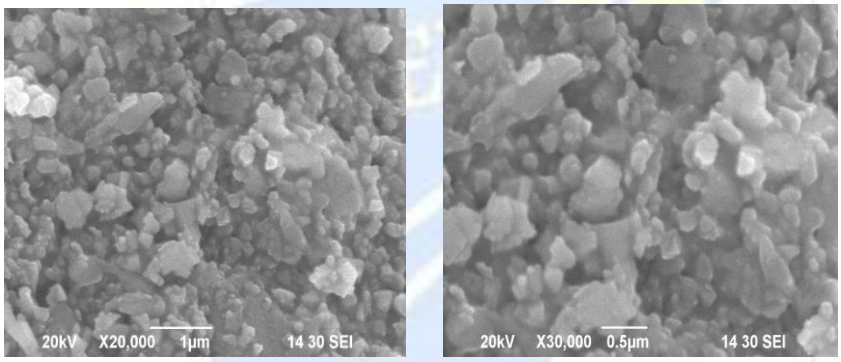

Fig 1.2: SEM micrograph of Mn_3O_4 nanoparticle

The chemical and elemental composition of the synthesized Mn_3O_4 nanoparticles can be verified by subjecting the samples for energy dispersive X-ray adsorption spectral studies. The EDAX patterns observed are shown in figure 1.3 and the compositions of elements, weight percentage and atom percentage in each sample are given in table 1.

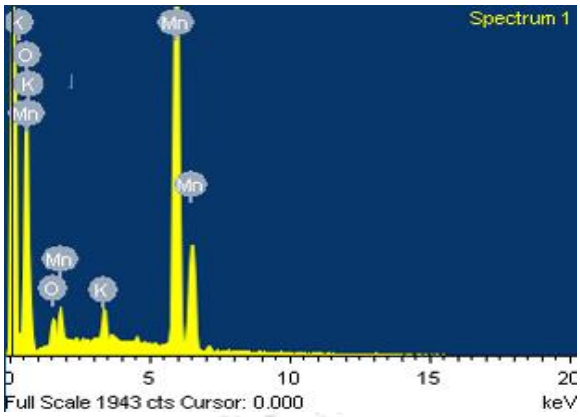

Fig1.3. EDAX of Mn_3O_4 nanoparticle

Element	Weight %	Atomic %
O K	41.90	72.19
K K	1.51	1.43
Mn K	56.59	26.38

Table 1: Elemental composition of Mn_3O_4 nanoparticle

Higher the intensity, higher will be the concentration of element in the sample. The EDAX pattern shows in which shell the element is present (K, L ...). The presence of feeble or trace amount of the element can also be traced out. The patterns match well with literature data (Chang et al. 2004, Banis et al. 2010). The EDAX pattern indicates that the nanoparticles are mainly composed of manganese and oxygen.

3.3 UV-Visible Spectroscopy

The optical absorption spectra of Mn_3O_4 nanocrystals are shown in figure 1.4. The spectrum reveals that both the samples absorb heavily in the visible region but moderately in the UV region. The high absorbance of light in the visible region indicates the applicability as an absorbing material that makes the material a good candidate in screening off UV portion of electromagnetic spectrum which is dangerous to human health.

Figure 1.4 shows the Tauc's plot of nano Mn_3O_4. The obtained value of E_g is tabulated in the table 1.2. The obtained band gap values suggest that the material is a semiconductor. The bandgap values are slightly lower than that reported byAnupam et al for Mn_3O_4 nanocrystal (Anupam et al 2013). Morphologies, crystalline degree and structural order disorder may play the role in the gap. The reduction in bandgap values attained may be due to the

structural disorder caused by the oxygen deficiency in the sample. Inorder to examine the effect of annealing on bandgap, the sample is annealed at 740 ℃. It has been found that the bandgap energy increases to some extend with increase in temperature. The obtained value for annealed sample is 2.71eV. The obtained value is well agreeing with the reported ones for tetragonal Mn_3O_4 (Pishdadian et al. 2012, Yokogawa et al. 1977).

The optical band of Mn_3O_4 nanocrystals synthesized by solvothermal process was reported to be of 3.21eV(Dubal et al 2010). The band gap value obtained in the present work may be attributed to the hydrous content in the material. The presence of water content was already pointed out in the vibrational analysis. Thus bandgap calculation indicates the rightness of our argument.

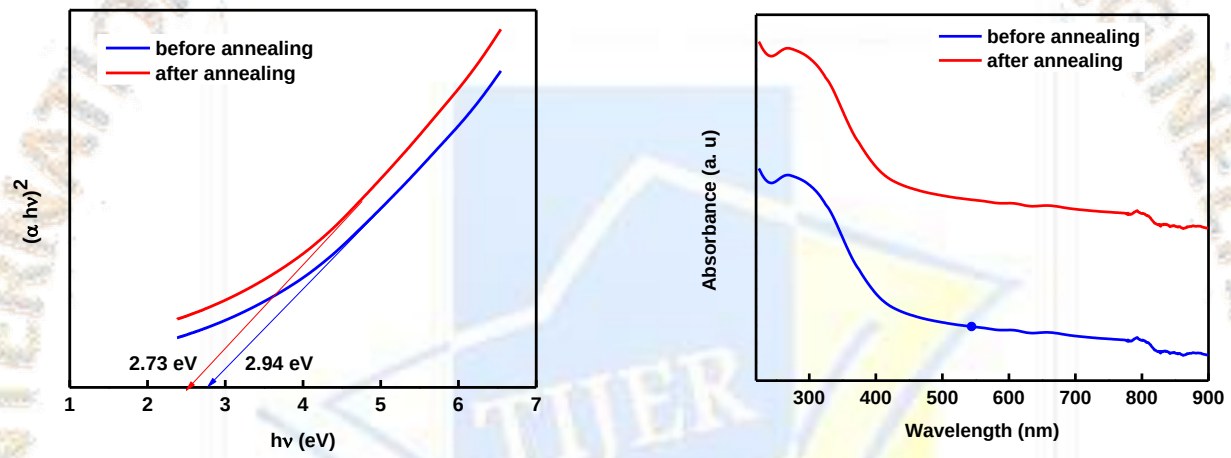

Fig: 1.4 UV –Vis spectra and Tauc's plot for Mn_3O_4 nanoparticles

3.4 Electrochemical Studies

The capacitive performance of manganese oxides was characterized by using cyclic voltammetry. The cyclic voltammograms of different manganese oxide electrodes were measured in 1M Na_2SO_4 electrolyte, at the scan rates of 100, 50, 25, 10, 5 and 2 mV/S respectively. The electrochemical performance of Mn_3O_4 nanoparticles were evaluated as a supercapacitor electrode in view of their intrinsic properties and unique structural features. Figure 1.5 shows the CV analysis at different scan rates with a potential range of 0.1 to 0.9 V.

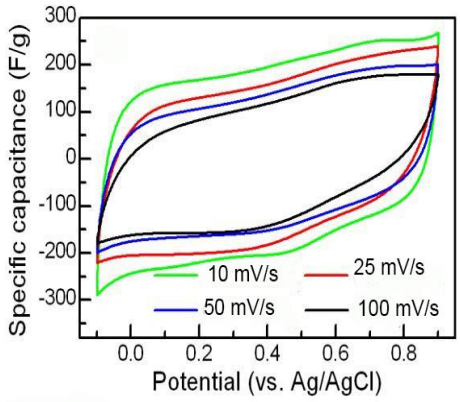

Fig 1.5: Cyclic Voltammetry curve of Mn_3O_4 in Na_2SO_4 electrolyte.

The CV curves at slow scan rate represent an ideal capacitive behavior with the rectangular shape. The deviation from rectangularity of the CV becomes distinct with increase of the scan rate. No obvious redox peaks are present in the CV curve, which reveals that the measured electrode is charged and discharged at a pseudo-constant rate over the complete voltammetric cycle. The Na^+ion from the electrolyte could occupy almost all the pores present in and on the Mn_3O_4 electrode surface; at a slower scan rate, this may result in the better and effective utilization of Mn_3O_4 for redox reaction in conjunction with good capacitance.The deposited oxide showed notably high specific capacitance resulting in its relatively smooth surface. The probable cause for high crystallinity exhibited could be the porous microstructure of Mn_3O_4.

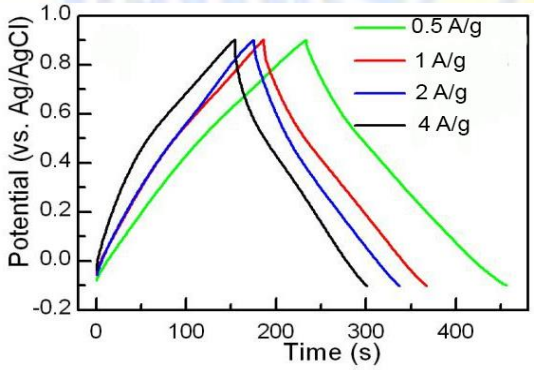

Fig 1.6: Galvanostatic charge – discharge curve of Mn_3O_4 in Na_2SO_4 electrolyte.

The capacitive performance of the as-synthesized sample was also investigated by using the charge-discharge method and the result of Mn_3O_4 is shown in figure 1.6. The specific capacitance of the electrode at different current densities can be calculated from the following equation,

$$C = \frac{Q}{\Delta V x W} = \frac{1}{2.\Delta V} \int \frac{W}{v.w} \, dI$$

Where C is the specific capacitance of the electrode based on the mass of active materials (F/g), Q is the sum of anodic and cathodic voltammetric charges on positive and negative sweeps. I is the sample current (A), W is the weight of active material (g) and V is the total potential deviation of the voltage window (V), V is the scanning rate (V/s) and W is the mass of active electrode materials (g). The charge discharge curve of Mn_3O_4 at different current densities depicts an almost equilateral triangle shape that reflects an ideal behavior. The corresponding specific capacitances at current densities of 4, 2, 1 and 0.5 A/g were calculated to 70, 90, 120 and 170 F/g respectively, which are superior to the reported values in literatures.

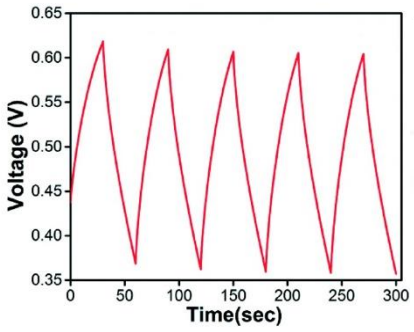

Fig 1.7: Potential vs. Time curve of Mn_3O_4.

Figure 1.7 shows the charge/discharge curves of Mn_3O_4 at current density of 0.5 A/g in a potential range of 0.35 to 0.65 V in 1M Na_2SO_4 electrolyte. A good linear relation of potential against time is regarded as a typical feature of an ideal capacitor. The Mn_3O_4curve is symmetric and linear for both charge and discharge portions, indicating that the electrodes have good capacitive behaviors with very sharp responses and small internal resistance (IR) drop. The charge curves are very symmetric to the corresponding discharge counterparts in the employed potential region;the slope of the curve is potential independent and maintains a constant value at the selected current density.

The variation in specific capacitance with current density curve for the Mn_3O_4 sample is shown in figure 1.8. Generally for the all compounds, as the current density increases, the specific capacitance increases and then decreases reaches a constant value. The lesser values of capacitance at high current rates is because of the less ionic penetration in the electrode surface when compared to the case at a low current rate. As expected, the capacitance of the cell decreases linearly with increasing current densities, which is the typical behaviour of electrochemical supercapacitors.

At the current density of 4 A/g the Mn_3O_4 electrode showed about 56% of the initial capacitance displayed a suitable capacitive retention. The effect of current density on specific capacitance is caused

by the transport of effective ions into active materials. The large current density allows charging process to be finished in a short time for higher concentration polarization (Chin et al. 2010, Devaraj and Munichandriah 2008). At a high current density,the retarding redox transitions of electroactive species would be exhausted by the protons in the vicinity of electrode/electrolyte interface. This necessity of specific capacitance upon current density is owing to the circumstance that electrochemical double layer capacitance is the foremost involvement to the observed overall capacitance.

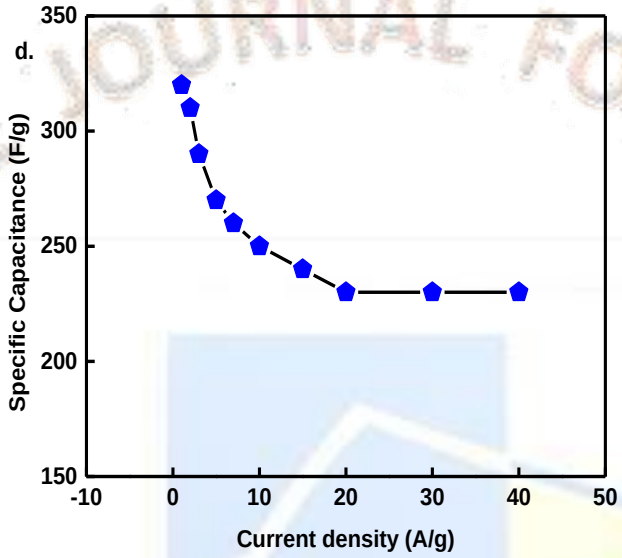

Figure 1.8 Specific capacitance vs current density curve of Mn_3O_4 in Na_2SO_4 electrolyte.

The specific capacitance versus scan rate for MnO, MnO_2, Mn_2O_3 and $Mn_3O_4$is shown in the figure 1.9

The Mn_3O_4 nanoparticle showed a specific capacitance of 211 F/g for a scan rate of 1mV/s. There is an increase in the specific capacitance when the scan rate at 1 mV/s. Beyond 1 mV/s, the specific capacitance decreases very slowly and displays almost persistent at higher scan rate. It is evident that the specific capacitance of Mn_3O_4 is greater at a lower scan rate and a constant decrease in specific capacitance is observed when compared with the other. This explains that the electrode is ideal and it can be used for high power applications.

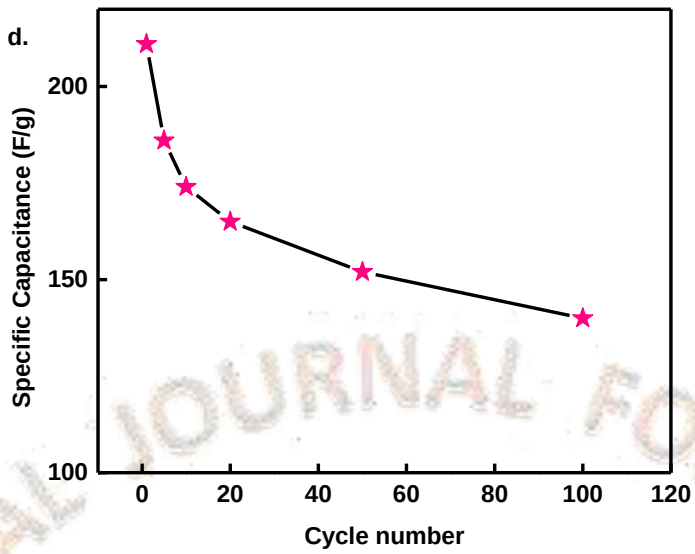

Figure 1.9 Specific capacitance vs scan rate of Mn_3O_4in Na_2SO_4electrolyte.

The specific capacitance versus cycle number for Mn_3O_4 is shown in the figure 1.10.

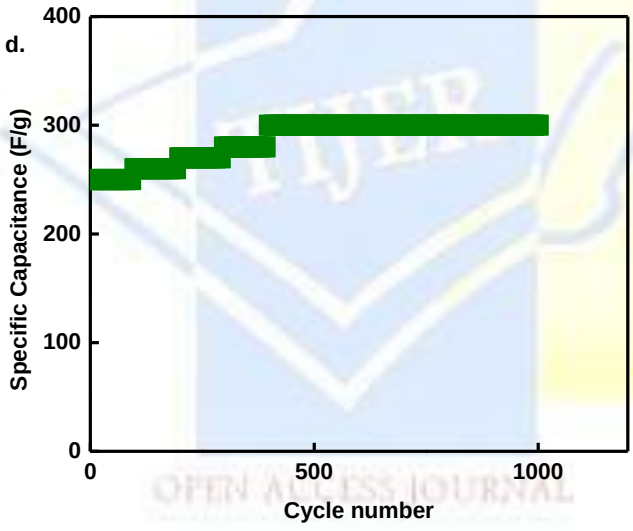

Figure 1.10 Specific capacitance vs cycle number of Mn_3O_4 in Na_2SO_4 electrolyte.

It is obvious from the figure that the specific capacitance remains nearly constant at the beginning 250 F/g then abruptly jumps to a higher value after 50 cycles. The specific capacitance value increases up to a maximum value from 256.1 F/g to 350 F/g, then subsequently decreases slightly and becomes nearly constant at the end of 1500 cycles. It is fascinating that the specific capacitance increases nearly 2.6 times after 50 cycles. This phenomenon is suggestive of the fact that there is an initial activation process for the

Faradaic pseudo capacitance for Mn/Na_2SO_4 electrodes. After 200 - 500 cycles specific capacitance decreases only 1.5% of the maximum value of capacitance. This decrease of capacitance can be attributed to the mechanical expansion of the manganese oxide nano layer due to the continuous ion insertion/desertion process or dissolution of some amount of manganese oxides into electrolyte (Beadrouet et al. 2009). Though, the electrolyte remains transparent after 1000 cycles, representing minimal dissolution of oxides into the electrolyte solution after the long-term cycling test which has been measured as the main reason behind the capacitance loss of manganese oxide-based supercapacitors.

The relationship between the capacitive retention and the cycle number is shown in figure 1.11. To assess the long-time cycling stability of Mn_3O_4, the capacitive retention was measured by continuous charge/discharge experiment at a current density of 3.0 A/g.

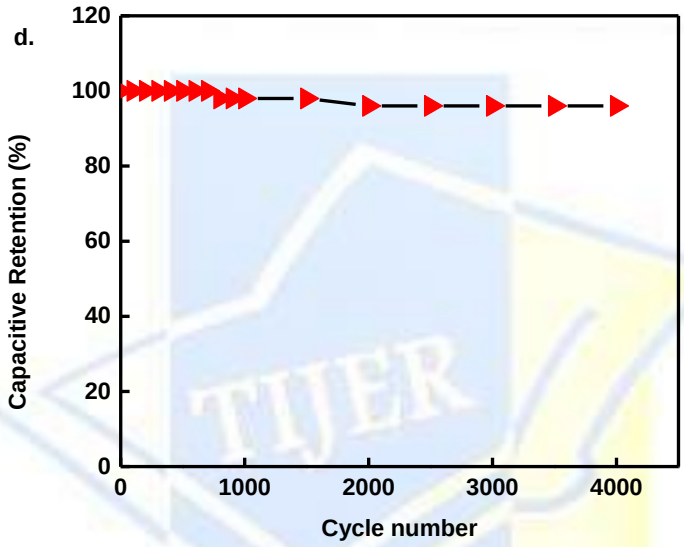

Figure 1.11 Capacitive retention vs cycle number of Mn_3O_4in Na_2SO_4 electrolyte.

After 1200 cycles, the capacitive retention for Mn_3O_4 is about 75 %, indicating an acceptable stability. In the first 300 cycles, the capacitive retention quickly decreases to about 56 %. Then, the capacitance is nearly constant with a capacitive retention of about 55% after 1200 cycles.

The CV curves are approximately symmetric in nature, and the curves after 50 cycles are nearly overlapping which signifies good cyclic capability of the nanocomposite pseudocapacitor (Nam 2006, Nalwa 2002, Shinomiya et al. 2005)). Therefore, this study suggests that the Mn_3O_4 nanocomposite is suitable for making electrode which shows good stability during the long-term cycling test.

4. Conclusion

Nanocrystalline semiconducting Mn_3O_4 was synthesized through the modified single step combustion process. The X-ray diffraction studies showed that the as-prepared Mn_3O_4 is single phased with tetragonal structure having crystalline size in the range 40-45nm. SEM image of the sample shows densification of the material with little porosity. The EDAX pattern confirms that the prepared nanopowder has elemental composition of Mn^{2+}, Mn^{3+} and O^{2-} in Mn_3O_4 micrograph. The uv-visible study showed that all the samples absorb maximum in the UV region. The absorbance spectra of the sample showed an extension to the visible region. Thus, these materials are ideal as coatings and manufacturing dyes. The obtained band gap value is 2.71eV for Mn_3O_4, which agrees well 0with the reported value for a perfect crystalline structure. The CV curve for Mn_3O_4 showed thatan ideal capacitive behaviour with the rectangular shape is detected for a slow scan rate.No redox peaks are observed which reveals that the electrode is charged and discharged at a pseudo constant rate.The charge/discharge curve at various current densities presented a specific capacitance of 70-170 F/g. The capacitive retention of Mn_3O_4 electrode showed about 86% of the initial capacitance. The specific capacitance against scan rate showed specific capacitance from 180-85F/g for 2-50mV/S.It can be concluded that different oxides of manganese can be used as a supercapacitor material in which MnO_2 and Mn_3O_4 gives good reversibility in the CV curve and good cyclability with efficient capacitive retention.

References

[1]Anilkumar. M. and Ravi. V. (2005) "Synthesis of nanocrystalline Mn_3O_4 at 100^0C", Materials Research Bullettin 40(4), 605 – 609.

[2] Dhaouadi. H., Madani. A. and Touati. F. (2010) "Synthesis and spectroscopic investigations of Mn_3O_4 nanoparticles", Materials Letters 64(21), 2395 – 2398.

[3] Donne. S. W. (2010) "Structure, morphology and electrochemical behavior of manganese oxides prepared by decomposition of permanganate", Journal of Power Sources 195(1), 367.

[4] Du. C., Yun. J., Dumas. R. K., Yuan. X., Liu. K. and Browning. N. D. (2008) "Three dimensionally intercrossing Mn_3O_4 nanowires", Acta Materialia 56, 3516 – 3522.

[5] Du. J., Gao. Y., Chai. L., Zou. G., Li. Y. and Qian. Y. (2006) "Hausmannite Mn_3O_4 nanorods: Synthesis, characterization and magnetic properties", Nanotechnology 17, 4923 – 4928.

[6] Dubal. D. P., Dhawale. D. S., Salunkhe. R. R., Fluari. V. J. and Lokhande. C. D. (2010) "Chemical synthesis and characterization of Mn_3O_4 thin films for supercapacitor application", Journal of Alloys and Compounds 497, 166 – 1770.

[7] Dubal. D. P., Dhawale. D. S., Salunkhe. R. R., Pawar. S. M. and Lokhande. C. D. (2010) "A novel chemical synthesis and characterization of Mn_3O_4 thin film for supercapacitor application", Applied Surface Science 256(14), 4411 – 4416.

[8] Dubal. D. P., Dhawale. D. S., Gujar. T. P. and Lokhande. C. D. (2011) "Effect of different modes of electrodeposition on supercapacitive properties of MnO_2 thin films", Applied Surface Science 257, 3378 – 3382.

[9] Vipin. C. Bose. and Biju. V. (2015) "Optical, electrical and magnetic properties of nanostructured Mn_3O_4 synthesized through a facile chemical route", Physica E 66, 24 – 32.

[10] Rao. C. N. R., John Thomas. P. and Kulkarni. G. U. (2008) "Nanocrystals: Synthesis, Properties and Applications", Springer, Germany.

[11] Durmus. Z., Tomas., Baykal. A., Kavas. H. and Toprak. M.S. (2011) "PEG-Assisted synthesis of Mn_3O_4 nanoparticles: A structural and magnetic study", Synthesis and Reactivity in inorganic, metal-organic and nano-metal chemistry 41(7), 768 – 773.

[12] Rao. C. N. R., Muller. A. and Cheetham. A.K (2007) "Chemistry of nanomaterials: Synthesis, Properties and Applications", Wiley – VCH, Weinheim.

[13] Yang Gogorsi (2006) "Nanomaterials Handbook", CRC Press, Taylor and Francis Group.

[14] Yang. L. X., Liang. Y., Chen. H., Meng. F. and Jiang. W. (2009) "Controlled synthesis of Mn_3O_4 and $MnCO_3$ in a solvothermal system", Materials Research Bulletin 44, 1753 – 1759.

[15] Yokogaw.M., Taniquchi. K. and Hamaguchi. C. (1997) "Fine structures in optical absorption spectra of MnO", Journal of the Physical Society of Japan 42, 591 - 595.

[16] Zhang. Y., Li. G., Lv. Y., Wang. L., Zhang. A., Song. Y. and Huang. B. (2011) "Electrochemical investigation of MnO_2 electrode material for supercapacitors", International Journal of Hydrogen Energy 36(11), 760 – 766.

[17] Zhang. Z., Sun. H., Shao. X., Li. D., Yu. H. and Han. M. (2005) "Three dimensionally oriented aggregation of a few hundred nanoparticles into monocrystalline architectures", Advanced Materials 17(1), 42 – 47.

[18] Sherin. J. S., Thomas. J. K. and Suthagar. J. (2014) "Combustion Synthesis and Magnetic Studies of Hausmannite, Mn_3O_4, nanoparticles", International Journal of Engineering Research and Development 10(7), 34 - 41.

[19] Sherin. J. S., Shiney Manoj. D., Haris. M. and Thomas. J. K. (2015) "Facile Synthesis and Characterization of Pyrolusite, β- MnO_2, Nano Crystal with Magnetic Studies", International Journal of Science and Engineering Applications 4(5), 2319-7560.

[20] Vidya. S., Solomon. S. and Thomas. J. K. (2013) "Synthesis, Characterization and low temperature sintering of nanostructured $BaWO_4$ for optical and LTCC applications", Advances in Condensed Matter Physics 2013, 409620.

[21] James. J., Jose. R., John. A. M. and Koshy. J. (2004) US Patent 6761866.

[22] James. J., Jose. R., John. A. M. and Koshy. J. (2004) US Patent 6835367.

[23] Vidya. S., John. A., Solomon. S. and Thomas. J. K. (2012) "Optical and dielectric properties of $SrMoO_4$ powders prepared by the combustion synthesis method", Advances in Materials Research 1, 191 – 204.

[24] Vidya. S., Solomon. S. and Thomas. J. K. (2012) "Synthesis, sintering and optical properties of $CaMoO_4$: A promising scheelite LTCC and photoluminescent material", Physica status solidi 209, 1067 – 1074.